Electronic Supporting Information

Proportion of Composition in a Composite does Matter to Behave as an Advanced Supercapacitor

Ramkrishna Sahoo[†], Anjali Pal[§] and Tarasankar Pal*[,†]

[†]Department of Chemistry, and [§]Department of Civil Engineering, Indian Institute of Technology, Kharagpur-721302, India

E-mail: *tpal@chem.iitkgp.ernet.in*

S1. A. Materials: All reagents were AR grade. Nickel acetate ($Ni(CH_3COO)_2$, $4H_2O$), ammonium monovanadate (NH_4VO_3) and sodium nitrate ($NaNO_3$) were purchased from E-Merck. Anhydrous ferric chloride ($FeCl_3$), potassium permanganate ($KMnO_4$), urea were purchased from Spectrochem. Ni foam, multiwalled carbon nanotube (MWCNT), graphite powder and polyvinylidene fluoride (PVDF) were purchased from Sigma-Aldrich. Acetylene black was purchased from Alfa aesar. Doubly distilled water was used to wash all the glassware and to prepare the solutions.

B. Characterization:

Powder X-ray diffraction (XRD) was carried out with a BRUKER-AXS-D8-ADVANCE diffractometer (Cu target). The XRD data analysis was performed using JCPDS software. The X-ray photoelectron spectroscopic (XPS) analysis was performed with VG Scientific ESCALAB MK II spectrometer equipped with a Mg Kα excitation source (1253.6 eV) and a five-channeltron detection system to analyse the oxidation state of the elements. The field emission scanning electron microscopic (FESEM) analysis was done with FEI NOVA NANOSEM 450 and the EDAX machine (BRUKER EDS microanalyzer) attached to the instrument was used to carry out the compositional analysis of the materials (IYC grant from DST). The transmission electron microscopic (TEM) analysis was carried out in a Hitachi H-9000 NAR instrument using an accelerating voltage of 300 kV. Electrochemical study was done using CHI 660E electrochemical work station. The effective BET surface area was performed using a Quantachrome ChemBET analyzer. The thermo gravimetric analysis (TGA) was performed using a PerkinElmer Pyris Diamond TG-DTA under atmospheric pressure.

S2: Calculation details for the electrochemical analysis:

Specific capacitance in three-electrode system, $C_{SP} = it/m\Delta V$ ---------- (1)

Specific capacitance in two-electrode system, C_{SP} (2 electrode cell) = $4\times C_{SP}$ ----------(2)

Where, I denotes the constant cathodic current, t signifies the discharge time, m is the weight of the active mass and ΔV is the potential window.

Coulombic efficiency, $\eta = t_D/t_C \times 100$ ---------- (3)

t_D is the discharging time and t_C is the charging time.

Energy density, $E=1/(2\times3.6)C_{SP}\Delta V^2$

Or

$$E = \left(\int_{t1}^{t2} iVdt\right) = \frac{1}{2} C (V_{max} + V_{min}) (V_{max} + V_{min})$$ ---------- (4)

Power density, $P= (3600\times E)/T$ ---------- (5)

Where, C denotes the specific capacitance at specific current, I is the discharge current and ΔV is the potential window, and T is the discharge time.

S3: Synthesis of graphene oxide using Hummers method:

We synthesized graphene oxide from graphite using Hummers method.[S1] Briefly, Pristine graphite was taken as the precursor and was oxidised by strong oxidizing agents, $KMnO_4$, $NaNO_3$ and conc. H_2SO_4. After that H_2O_2 was added to the mixture to remove the excess $KMnO_4$ and to convert the generated MnO_2 to $MnSO_4$. Then it was washed with hot water and air dried. After that 50 mg of the solid material was dispersed with 50 mL distilled water through sonication for 3 h and then it was centrifuged for 30 min at 3000 rpm speed for washing. Finally the solid was dispersed in water and the solution was taken and used for the preparation of different β FeOOH@rGO composites.

S4: Table:

Electrode	Performances	Reference
1. Fe_3O_4-rGO	Specific capacitance 661 F/g at 1 A/g.	S2
2. rGO@Fe_3O_4	Specific capacitance 316 F/g at 1 A/g	S3
3. FeOOH	Specific capacitance 116 F/g at 0.5 A/g	S4
4. $ZnFe_2O_4$	Specific capacitance 1235 F/g at 1 mA/cm^2	S5
5.$MnFe_2O_4$	Specific capacitance 99 F/g	S6
6. Fe_2O_3@rGO	Specific capacitance 472 F/g at 0.5 A/g.	S7
7. Iron nanosheet on graphene	Specific capacitance 717 F/g at 2 mV/s, poor stability	S8
8. Graphene @CNT@FeOOH	Specific capacitance 267 F/g at 0.5 A/g, low rate capability	S9
9. β FeOOH@rGO	Specific capacitance 1306 F/g at 1 A/g	Present work

Table S1: Comparison of the specific capacitance values for different iron based pseudocapacitor electrodes.

S5: Figures:

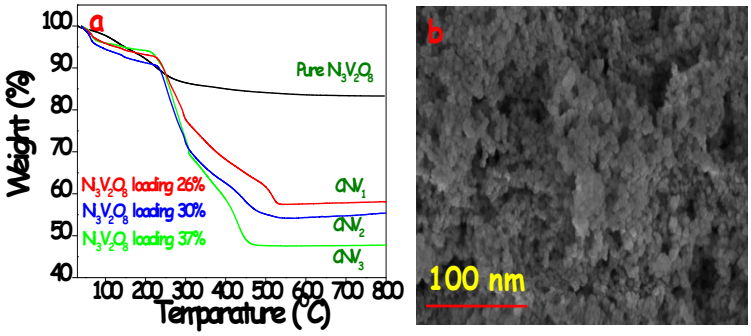

Figure S1: (a) TG curve of the pure $Ni_3V_2O_8$ NPs and its composites and (b) FESEM image of pure $Ni_3V_2O_8$ NPs.

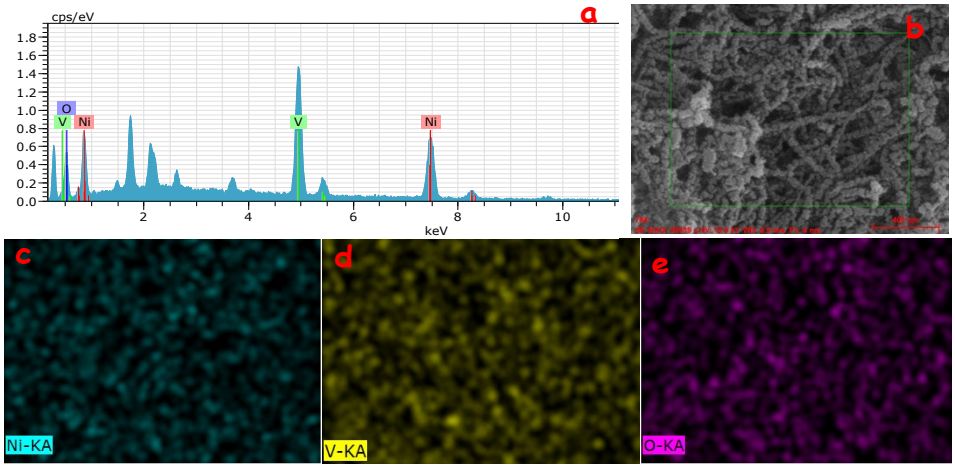

Figure S2: (a) EDX and (b) elemental area mapping of the CNV composite.

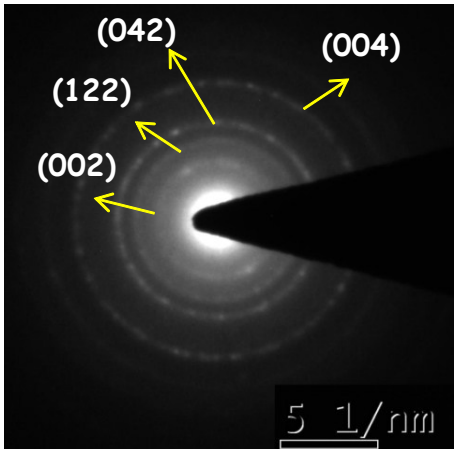

Figure S3: Selected area electron diffraction (SAED) pattern of the CNV composite.

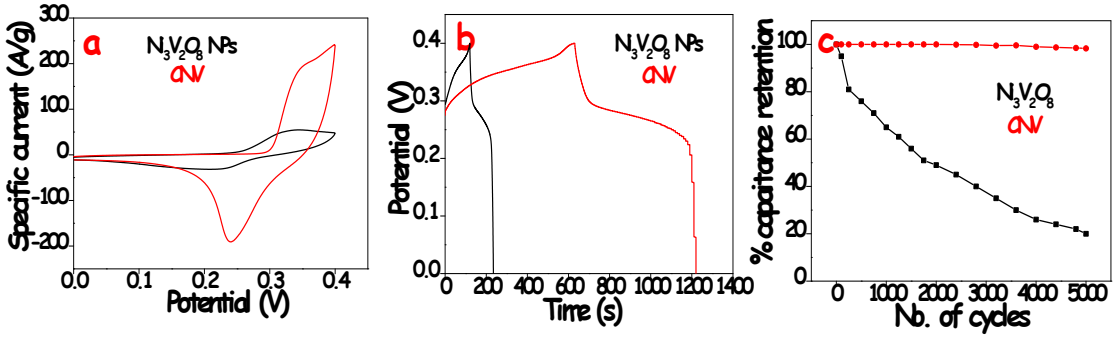

Figure S4: Comparative (a) CV curves, (b) charge-discharge curves and (a) cyclic stability up to 5000 charge-discharge cycles studies of pure $Ni_3V_2O_8$ NPs and CNV composite**.**

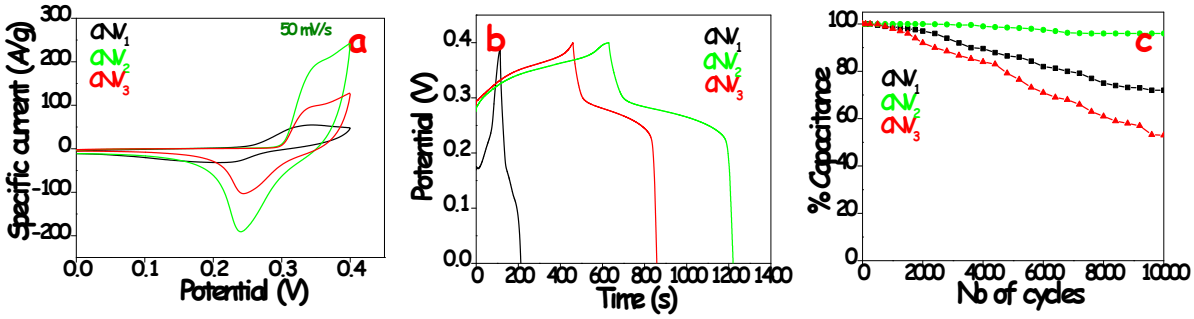

Figure S5: Comparative (a) CV curve, (b) charge-discharge curve and (c) cyclic stability up to 10000 cycles studies of CNV_1, CNV_2 and CNV_3 composites.

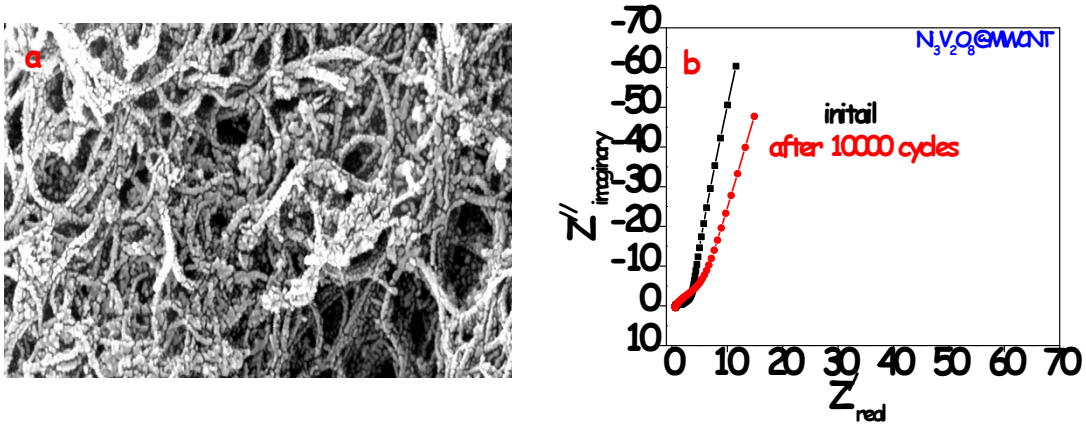

Figure S6: (a) FESEM image after 10000 charge-discharge cycles and (b) Nyquist plot (initial and after 10000 charge-discharge cycles) of the CNV composite.

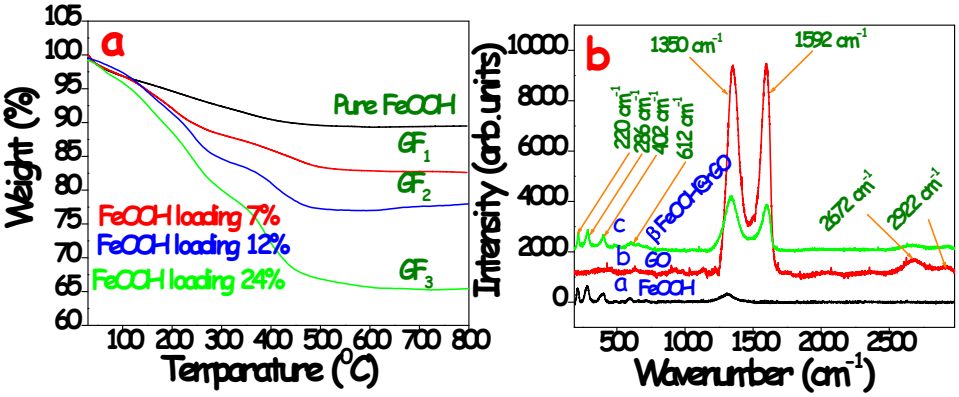

Figure S7: (a) Comparative TG curves of pure FeOOH nanorods and its composites and (b) comparative Raman spectra of pure FeOOH, GO and GF composite.

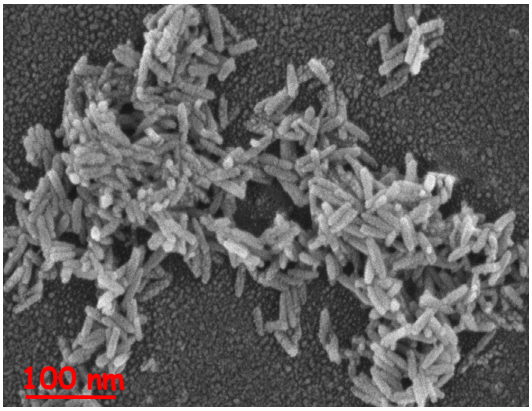

Figure S8: FESEM image of pure FeOOH nanomaterials.

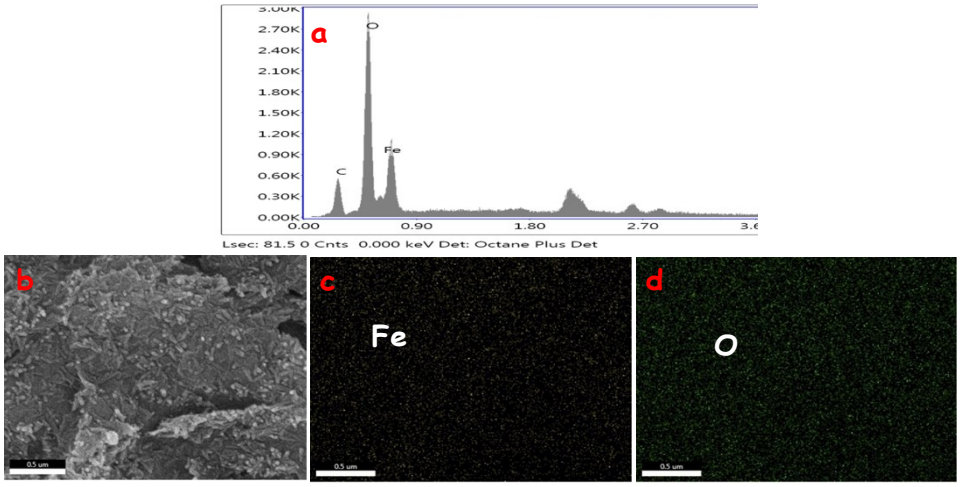

Figure S9: (a) EDX spectra and (b) elemental area mapping of the GF composite.

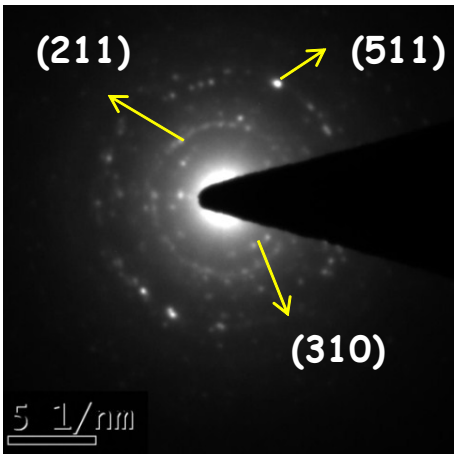

Figure S10: SAED pattern of the GF composite.

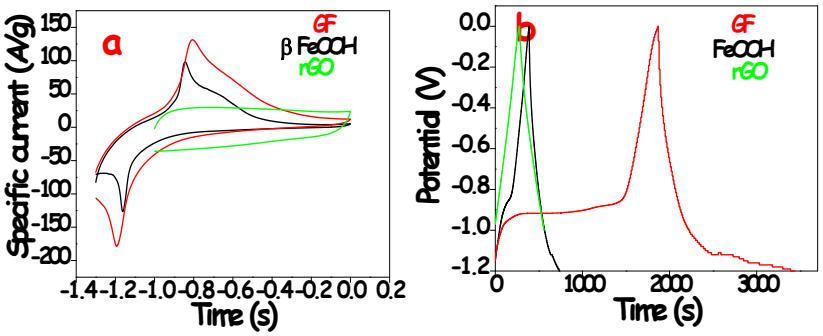

Figure S11: Comparative (a) CV curves and (b) charge-discharge curves of the GF composite, pure FeOOH and rGO.

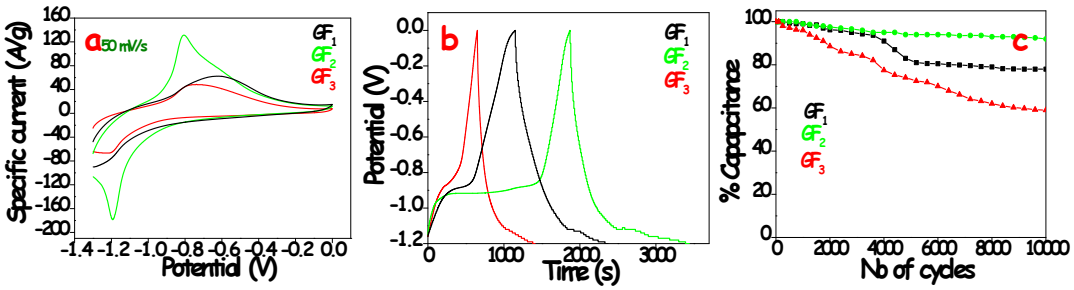

Figure S12: Comparative (a) CV curves, (b) charge-discharge curves and (c) cyclic stability up to 10000 charge-discharge cycles of the GF_1, GF_2 and GF_3 composites.

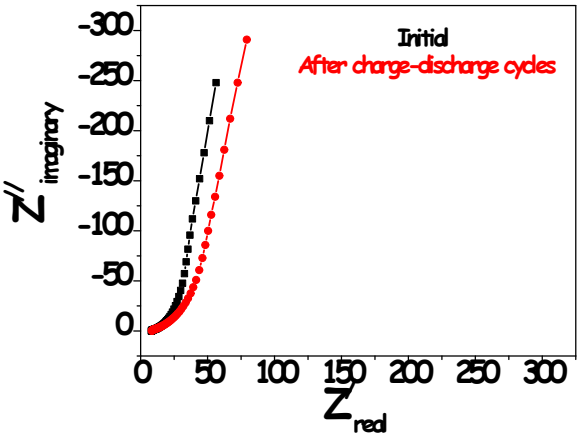

Figure S13: Nyquist plot (initial and after 10000 charge-discharge cycles) of the GF composite.

References:

S1. Hummers, W. S.; Offeman, R. E. J. Am. Chem. Soc. 1958, **80**, 1339.

S2. T. W. Lin, C. S. Dai and K. C. Hung, *Sci. Rep.*, 2014, **4**, 7274.

S3. J. Zhu, L. Huang, Y. Xiao, L. Shen, Q. Chen and W. Shi, *Nanoscale*, 2014, **6**, 6772–6781.

S4. W. H. Jin, G. T. Cao and J. Y. Sun, *J. Power Sources*, 2008, **175**, 686–691.

S5. T. Cottineau, M. Toupin, T. Delahaye, T. Brousse and D. Belanger, *Appl. Phys. A*, 2006, **82**, 599–606.

S6. A. Shanmugavani and R. K. Selvan, *RSC Adv.*, 2014, **4**, 27022–27029.

S7. Y. P. Lin and N. L. Wu, *J. Power Sources*, 2011, **196**, 851–854.

S8. J. J. Li, M. C. Liu, L. B. Kong, D. Wang, Y. M. Hu, W. Han and L. Kang, *RSC Adv.*, 2015, **5**, 41721 41728.

S9. C. Long, T. Wei, J. Yan, L. Jiang and Z. Fan, *ACS Nano*, 2013, **7**, 11325–11332.